Lutidine-Based Ionic Liquids for Efficient Dissolution of Cellulose ~~for~~ and its Applications: Pprocessing and Mmodifications

[a]Rakesh Samikannu*, [a]Shashi Kant Shukla, [a]Ajaikumar Samikannu, [a,b]Jyri-Pekka Mikkola*

[a]*Umeå University, Department of Chemistry, Chemical-Biology Centre, Technical Chemistry, SE-90787 Umeå, Sweden;*

[b]*Åbo Akademi University, Process Chemistry Centre, Laboratory of Industrial Chemistry and Reaction Engineering, FI-20500 Turku, Finland.*

Abstract

Herein, we have studied the potential of lutidinium-based ILs (dialkylpyridinium-based ILs) containing chloride and acetate anions in the dissolution of cellulose. Surprisingly, only lutidinium chloride ~~showed activity in~~was able to dissolve~~ing~~ cellulose samples while lutidinium acetate ILs ~~remained inactive~~could not despite that their structure was confirmed by ^{1}H- and ^{13}C NMR spectra, resperctively. 1-allyl-3,5-dimethyl pyridinium chloride [3,5-ADMPy]Cl exhibited the highest ~~efficiency~~ capacity in cellulose dissolution. In fact, it dissolved 20 wt% of cellulose within 12 min and 30 wt% of cellulose in 35 min at, 120 ^{o}C. The crystallinity and morphology of native and regenerated cellulose were characterised by X-ray diffraction (XRD), scanning electron microscopy (SEM) and CP/MAS ^{13}C NMR spectroscopy. These techniques clearly suggest that the crystallinity of cellulose ~~go down~~is reduced upon treatment in lutidinium chloride. The thermo gravimetric analysis (TGA) showed that regenerated cellulose ~~has~~ had thermal stability close to that of ~~the~~ native cellulose.

Keywords: *X-ray diffraction, Cross polymerization/magic angle spinning ^{13}C NMR, Thermogravimetric analysis, viscosity, Scanning electron microscopy, Cellulose dissolution.*

Introduction

The increasing energy demand and the stricter environmental regulations urge the chemical industries to find alternative and renewable resources to provide cleaner energy and eliminate the dependency of fossil resources to produce value-~~-~~added products and platform chemicals.

In this context, lignocellulosic biomass ~~have~~ has been receiving much attention ~~from~~ during several decades for the reason that~~,~~ it is a non-edible, CO_2-neutral and most abundant renewable raw material that can be found widely distributed over the earth.[1-4] Among major components of lignocellulosic biomass, cellulose has attracted much attention because of its properties, such as biocompatibility, biodegradability, thermal and chemical stability and fascinating structural and physical properties.[5-7] Cellulose and its derivatives are found useful in many potential applications such as, fiber, paper, membranes, tissues, polymers and paint industries.[8-9] On the other hand, bio-fuel industries pay much attention to derive fuels, fuel precursors and platform chemicals from cellulose through enzymatic fermentation, catalytic fractionation, and hydrolysis/hydrogenation techniques[10-12]. However, the utilization of cellulose to ~~make~~ produce value~~-~~-added products ~~are~~ is not straightforward owing to its crystalline nature. Cellulose strands associate themselves strongly through the strongest inter- and intra-molecular hydrogen bonds that ~~affects~~ hampers solubility and processing of it in a medium. Cellulose is insoluble in most of the organic solvents but dissolves partially in strongly basic solvents or solvent systems such as, N-methylmorpholine-N-oxide (NMMO),[13] N- dimethylacetamide/lithium chloride (DMAC/LiCl),[14-18] 1,3-dimethyl-2-imidazolidinone/lithium chloride (DMI/LiCl),[19] and NaOH/Urea,[20] dimethyl sulfoxide/paraformaldehyde (DMSO/PF)[21-22], concentrated inorganic salt ($ZnCl/H_2O$, $Ca/SCN)_2/H_2O$, $LiClO_4.3H_2O$) and mineral acids (H_2SO_4/H_3PO_4)[23]. The use of these solvent systems in current industrial practices is posing several disadvantages such as chemical hazardousness, toxicity and large amount of waste generated during the processing. On the other hand, practical difficulties such as demand for harsh conditions, equipment corrosion, formation of by-products, difficulties~~y~~ in product separation, solvent recovery, process instability and handling difficulties also linger with these solvent systems.

In the recent years, ionic liquids (ILs) have been explored extensively in many applications owing to their exceptional physico-chemical properties and ability to ~~tune~~ to be

easily tailored. Ionic liquids are molten organic salts at room temperature (<100 ◦C) and typically consist of an organic cation and an organic/inorganic anion. The beneficial properties of the ILs such as low melting point, negligible vapour pressure, miscibility, non-volatility, thermal stability[24-27] and recyclability give them advantage over traditional solvents for various solvents including cellulose dissolution. The pioneering work of Rogers and co-workers showed that cellulose can be dissolved in hydrophilic IL 1-butyl-3-methylimidazolium chloride ([C_4mim]Cl) without any pre-treatment, and regeneration of ~~regenerated the dissolved~~ cellulose without any degradation can be performed by addition of water/antisolvent.[28] Since then, a number of ILs have been ~~studied~~ developed for cellulose dissolution, including those with halide, phosphonate, formate and acetate anions, along with pyridinium, imidazolium, morpholinium, and phosphonium cations.[29]

In the present study, we report four pyridinium-based ionic liquids namely, 1-allyl-3,4-dimethyl pyridinium chloride [3,4-ADMPy]Cl, 1-allyl-3,5-dimethyl pyridinium chloride [3,5-ADMPy]Cl, 1-allyl-3,4-dimethyl pyridinium acetate [3,4-ADMPy]OAc, and 1-allyl-3,5-dimethyl pyridinium acetate [3,5-ADMPy] OAc for the dissolution of cellulose. The above said ILs were synthesized at ambient conditions and characterized by means of FTIR and ^{1}H- and ^{13}C-NMR spectroscopic methods. The efficiency of synthesized ILs in the cellulose dissolution were studied at different reaction conditions. The changes in the morphology of native and regenerated cellulose were investigated using Scanning Eelectron Mmicroscopy (SEM), CP/MAS ^{13}C-NMR and X-ray Ddiffraction techniques (XRD). The thermal stability of the ILs before and after dissolution of cellulose was examined by means of Thermo Ggravimetric Aanalysis (TGA).

Experimental

Materials

3,4-Dimethyl pyridine, 3,5-dimethyl pyridine and allyl chloride were ~~procured~~ purchased from Sigma Aldrich and distilled prior to use. Sodium acetate (≥99.0%) and sodium carbonate

(≥99.8%) were obtained from Merck and used without further purification. Amberlite IR-400 OH resin was purchased from Sigma Aldrich and used without any pre-conditioning. Highly pure cellulose was obtained from Aditya Birla Domsjö AB (sulfite cellulose pulp). Micro-crystalline cellulose (MCC) was obtained from Sigma Aldrich Ltd.

Synthesis of ionic liquids

1-Allyl-3,4-dimethyl pyridinium chloride and 1-allyl-3,5-dimethyl pyridinium chloride

In a 250 mL three-necked round-bottomed flask was equipped a nitrogen inlet adapter, a reflux condenser with calcium chloride in a drying tube at the outer end of condenser and an addition funnel with a pressure-equalizer arm. The flask is flushed with nitrogen and charged with 100 ml acetonitrile along with 10 g (0.0933 mole) of distilled dimethyl pyridine. Subsequently, 8.6 g of allyl chloride (1.2 mole) was added drop-wise in the flask under vigorous stirring. The mixture was then allowed to refluxed at 60 °C for 12 h under nitrogen flow. The resultant solution was first washed with excess of dichloromethane and later placed over ultrahigh vacuum to remove water vapors and high boiling impurities. The remaining traces of impurities were removed by placing the ionic liquid ~~using~~ in a rotary evaporator equipped with a vacuum pump and conditioned at 70 °C for 6h. At the end, a white solid was obtained which ~~in~~ was ~~kept~~ inserted in air-tight bottles and stored in desiccator under low pressure.

1-Allyl-3,4-dimethyl pyridinium acetate and 1-allyl-3,5-dimethyl pyridinium acetate

The acetate-based ILs were obtained by exchanging chloride anion from [3,4-ADMPy]Cl and [3,5-ADMPy]Cl by acetate anion using anion exchange rasin. 10g Amberlite IRA-400(R-OH) in deionized water was loaded in a 20×1.5 cm chromatographic column followed by passing 100 mL of 1M sodium acetate solution through the column at a flow rate of 1 mL/min. The column was then thoroughly washed with deionized water until the pH of the eluent was same as that of deionized water (pH ~7). Afterwards, 5g 1-allyl-3,4-dimethylpyridinium chloride was dissolved in 50 mL deionized water and the solution was passed through the column at a flow

rate of 1 ml/min followed by 50 ml of deionized water. The eluent was collected and evaporated and water was removed by freeze drying followed by placing the solution under vacuum at 70 °C for 6h. At the end 3.978 g of 1-allyl-3,4-dimethylpyridinium acetate was collected as a brown liquid. The 1-allyl-3,5-dimethylpyridinium acetate was prepared similarly. The different steps of IL preparation are shown in scheme 1.

The synthesized ionic liquids were characterized by NMR and FT-IR spectroscopy. ^{1}H and ^{13}C NMR spectra were recorded from Bruker AV 400 spectrometer and are shown as supporting information (ESI). The proton COSY spectrum of [3,5-ADMPy]Cl is shown in supporting information (ESI). The FT-IR spectra were obtained from Perkin Elmer FT-IR spectrometer equipped with Attenuated Total Reflection (ATR) capability. The water contents of the ionic liquids were measured by Metrohm 756 KF Coulometer. For SEM images, a small piece of cellulose film was prepared and examined using a Hitachi S- 3000H Japan in the voltage range 0.5-30 kV.

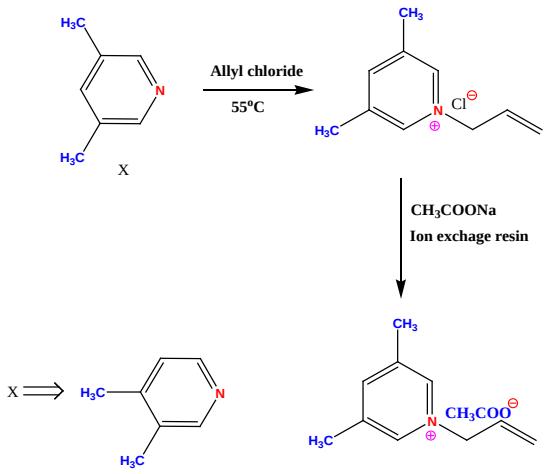

Scheme 1. Synthesis of ionic liquids.

Dissolution and regeneration of cellulose

Cellulose samples were dried at 60ºC in vacuum for 5h before use. In a 20 ml glass vial 5, 10, 15, 20, 25 and 30 wt% of cellulose samples in 1-allyl-3,5-dimethyl pyridinium chloride ([3,4-ADMPy]Cl) were added and heated in a oil bath 90ºC, 100ºC, 110ºC and 120ºC with continues stirring until a trasparent solution of cellulose was obtained. The progress of cellulose dissolution was monitored by polarized optical microscope. After complete dissolution of cellulose, transpar~~e~~nt viscous ionic liquid solution was casted on a glass plate under vacuum for removing bubbles. The glass plate was kept in 50 ml deionized water for 90 min. The regenerated film was thoroughly washed with water to remove ionic liquid completely followed by drying at 60ºC in a vacuum oven. The collected aqueous layer was evaporated under vacuum at 60 °C to obtain pure and dry ionic liquid.

Table 1. Dissolution of different cellulose (wt%) in lutidinium-based ILs at various temperatures and times. Sulfite cellulose (cell), cellulose (MCC)

Ionic liquids	**Cellulose**	**Temperature (ºC)**	**% Weight dissolved**	**Time (min)**
[3,5-ADMPy]Cl	Cell	120	10	8
		120	20	12
		120	32	40
	MCC (DP = 789)	120	5	10
		120	10	18
		120	15	27
		120	19	50
[3,4-ADMPy]Cl	Cell	110	5	10
		110	10	22
		120	5	8
		120	10	15
		120	15	35
		120	18	55
	MCC (DP = 789)	120	5	12
		120	10	21

		120	15	32
[3,5-ADMPy][CH_3COO]	Cell	120	-	-
	MCC (DP = 789)	120	-	-
[3,4-ADMPy][CH_3COO]	Cell	120	-	-
	MCC (DP = 789)	120	-	-

Results and discussion

The dissolution of two cellulose samples namely sulphite cellulose (Cell) and microcrystalline cellulose (MCC) ~~are~~ were performed in two ILs, namely 1-allyl-3,4-dimethylpyridinium chloride ([3,4-ADMPy]Cl) and 1-allyl-3,5-dimethylpyridinium chloride ([3,5-ADMPy]Cl) and results are shown in Table 1. In [3,5-ADMPy]Cl, 32 wt% of sulphite cellulose was dissolved in 40 min, whereas only 19 wt% of MCC could be dissolved at 120 ^oC. The snapshots of different sulphite cellulose samples (10, 20 and 32 wt%) in [3,5-ADMPy]Cl before and after dissolution are shown in Figure 1. Depending on the wt% of sulphite cellulose in [3,5-ADMPy]Cl, pale yellow to dark brown color was observed at the end of dissolution. It is evident from Table 1 that efficiency of ILs decreases with the increasing degree of polymerization of cellulose samples. Compared to [3,5-ADMPy]Cl, lower wt% of sulphite cellulose could be solubilize in [3,4-ADMPy]Cl even after longer treatment. Similarly for a given wt% of MCC at 120 ^oC, longer time was required with [3,4-ADMPy]Cl than that of [3,5-ADMPy]Cl. This anomality in the dissolution behavior of ILs probably arises due to the asymmetric substitution of methyl group on pyridinium cation. A symmetric substitution of methyl group on pyridinium cation results in greater dissolution of sulphite cellulose than those having asymmetric distribution of methyl group at same temperature and similar period of treatment. With the increasing wt% of cellulose samples viscosity of the solvated state also increase.

Surprisingly, 1-allyl-3,4-dimethylpyridinium acetate ([3,4-ADMPy][CH_3COO]) and 1-allyl-3,5-dimethylpyridinium acetate ([3,5-ADMPy][CH_3COO]) did not reveal any

activity when treated with cellulose samples. These observations seems quite unrealistic as acetate anion ([CH_3COO]) with various combinations of cation is reported as potential IL for cellulose dissolution because of its high basicity. The basicity of anion in an IL depends on the acidity of the complementary cation as suggested by the polarity study. The ^{1}H NMR chemical shift (δ) of acidic protons on cation due to the anion is a suitable parameter to detect the basicity of anion. A basic anion closely approach to the cation and causes higher deshielding to acidic protons than that of weakly acidic anion. The ^{1}H NMR spectra of chloride- and acetate-based ILs containing same cation show different chemical shift for acidic protons at 2, 4 and 6 (in [3,5-ADMPy]) positions and 2, 5 and 6 positions ([3,4-ADMPy]). All chloride-based ILs have higher chemical shift for acidic protons than acetate-containing ILs. This clearly revels that acetate act as a weak base when attached to the [3,5-ADMPy] and [3,4-ADMPy] cations. The lower basicity ~~makes~~ renders them inefficient for cellulose dissolution.

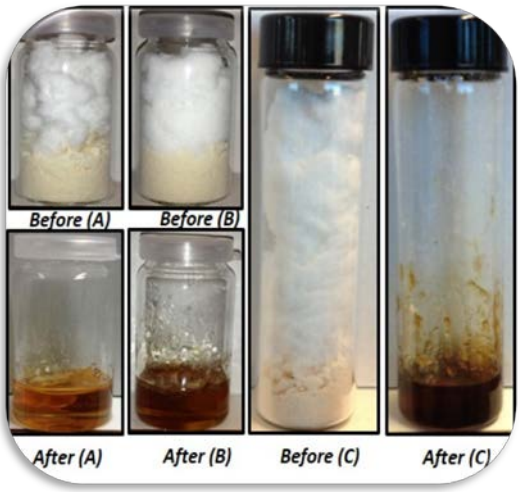

Figure. 1. Photograph of different amounts of cellulose dissolved in [3,5-AMPy]Cl at different temperatures before and after dissolution (a) 10 wt% cellulose at 120 ^{o}C, (b) 20 wt% cellulose at 120 ^{o}C, (c) 32 wt% cellulose at 120 ^{o}C.

The dissolution of cellulose was observed visually as well as using an optical microscope. As shown in Figure 2, cellulose lose its native structure upon dissolution in ILs. In the microscopic images, absence of cellulose fibers confirms the breakdown of the crystalline structure of cellulose at higher temperature in [3,5-ADMPy]Cl as exhibited in Figure 2 (B and C).

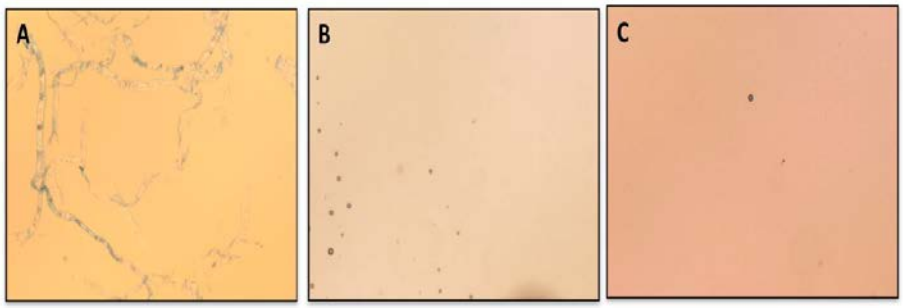

Figure 2. Optical micrographs of cotton cellulose at 100 µm for native cotton (A) and (B) at 100 µm for regenerated cellulose from [3,5 ADMPy]Cl and 1 µm magnification for regenerated cellulose (C).

Structure and morphology of regenerated cellulose films from [3,4-ADMPy]Cl and [3,5-ADMPy]Cl

The dissolved cellulose was regenerated upon addition of water as an anti-solvent. For various characterization, IL/cellulose solution was casted on a glass plate and dipped in water to remove IL. Subsequently, the film was removed from water and dried under ultra-low vacuum. The recovered cellulose was then characterized by scanning electron microscopy (SEM), wide-angle X-ray diffraction (XRD), cross polymerization/magic angle spinning (CP/MAS) ^{13}C NMR, thermogravimetric analysis (TGA), and Fourier transform infrared (FT-IR) spectroscopic methods.

The progress of dissolution in ILs was observed by monitoring the morphology of native and regenerated cellulose by SEM. Figure 3 illustrates SEM micrographs of native

and regenerated cellulosic forms. The recovered cellulose post dissolution becomes smoother, dense and uniform (Figure 3 (b) and (c)) than rough and scattetered surface of untreated cellulose samples (Figure 3(a)). These chages in the morphology indicate re-conglomeration of robust crystalline structure of cellulose fibers into less-compact/unwoven macromolecular assembly upon dissolution.

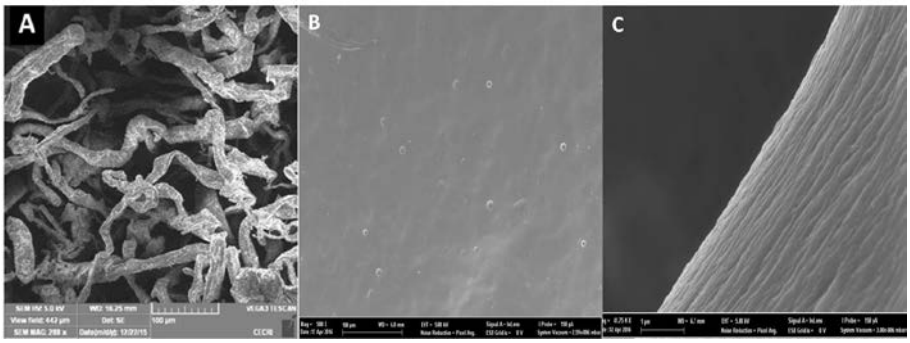

Figure 3. Optical and SEM micrographs of cotton cellulose at 100 µm for native cotton (a) and (b) at 100 µm for regenerated cellulose from [3,5-ADMPy]Cl and 1 µm magnification for regenerated cellulose (c).

Solid-state CP/MAS ^{13}C NMR spectra

In CP/MAS ^{13}C NMR of cellulose, C-4 and C-6 are indicative peaks of cellulose dissolution. Native cellulose shows characteristic peaks at 105.7 (C-1), 89.6 (C-4), 84.24 (C-4), 73.5 (C-5), 72.68 (C-2, C-3), 65.8 (C-6), and 62.93 ppm (C-6).[30,31] Upon dissolution, cellulose morphology changes around C-4 and C-6 peaks. In cellulose samples, signal at 89.15 ppm and 82.24 ppm are attributed to the C-4 and correspond to the crystalline and amorphous cellulose, respectively. The signals at 65.33 ppm and 62.93 ppm correspond to the crystalline and amorphous C-6, respectively. In regenerated cellulose samples, the signals at 89.14 ppm and 62.93 ppm were disappeared as evident from the CP/MAS ^{13}C NMR spectrum. The disappearance of the crystalline C-4 signal clearly indicate the breakdown of crystallinity. The shifting of C-6 signal in the regenerated cellulose film from 65.8 to 63.8 ppm suggest that the

"t-g" conformation of the C6-OH group, which is indicative of the crystalline nature, changes to "g-t" conformation, a characteristic of amorphous nature.[32] The decrease in the sharpness of CP/MAS ^{13}C NMR signals of native cellulose compared to that of regenerated cellulose fortify the reduction of the cellulose crystallinity. Moreover, the manifestation of signals at 77 and 107 ppm in the typical CP/MAS ^{13}C NMR spectrum of crystalline cellulose and regenerated sample further supports an amorphous structure. The absence of any other signal in the spectrum shows the efficacy of [3,5-ADMPy]Cl as a non-derivatizing and potential solvent for cellulose dissolution.

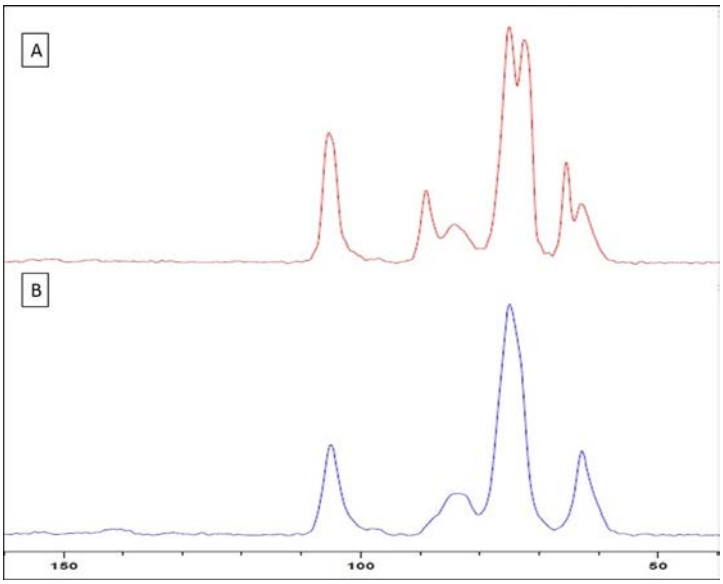

Figure 4. CP/MAS ^{13}C NMR spectra of native cellulose (a) and regenerated cellulose samples (b).

The preliminary observation of cellulose dissolution can be seen in the FT-IR spectrum. Both native and regenerated cellulose sample show broad peak due to O-H stretching between 3000-3600 cm^{-1}. The signal at 2887 cm^{-1} in all samples is owing to the C–H stretching

vibration.[33] The band at 1365 cm^{-1} is attributed to the O–H bending vibration and the strong band at 1020 cm^{-1} is the characteristic of C–O–C stretching. However, compared to the native cellulose regenerated cellulose exhibit broader peak at higher wavenumber (3432 cm^{-1}) as shown in Figure 5. The broadening of the –O-H peak at higher wavelength confirm the cleavage of H-bonding in the regenerated cellulose samples. An additional peak ~ 992 cm^{-1} in the regenerated cellulose was due to the C-O stretching vibration in the amorphous region. Furthermore, it could be observed that these spectra were quite similar and no new peaks appeared in the regenerated samples, indicating absence of any reaction between cellulose and ILs during the dissolution and regeneration processes. The FT-IR and CP/MAS ^{13}C NMR spectra clearly indicate the non-derivatizing nature of [3,5-ADMPy]Cl in the cellulose dissolution and regeneration.

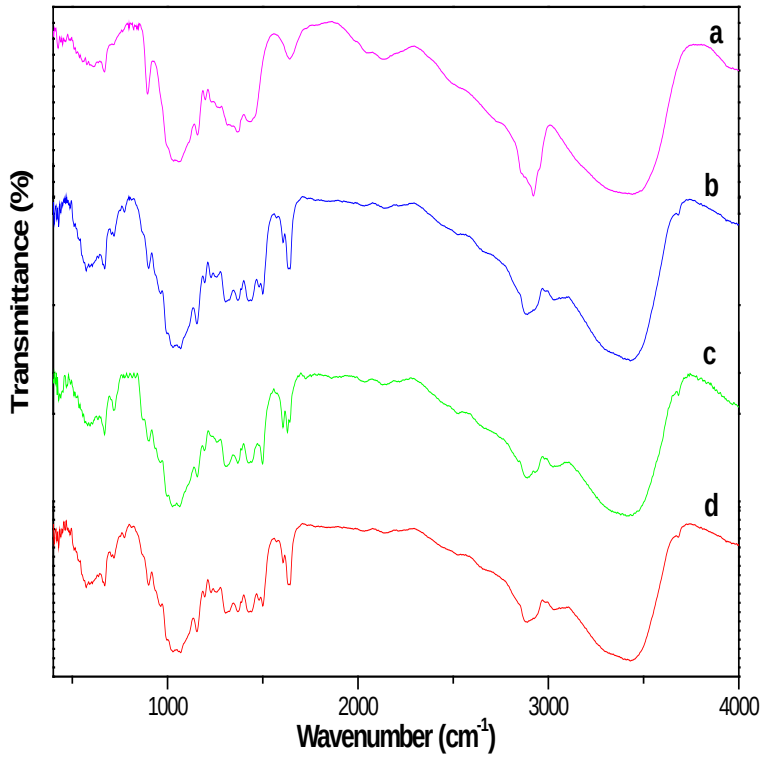

Figure 5. FT-IR spectra of native cellulose (a) and regenerated cellulose with 10 wt% (b) 20 wt% (c) and 32 wt% (d) from [3,5-ADMPy]Cl.

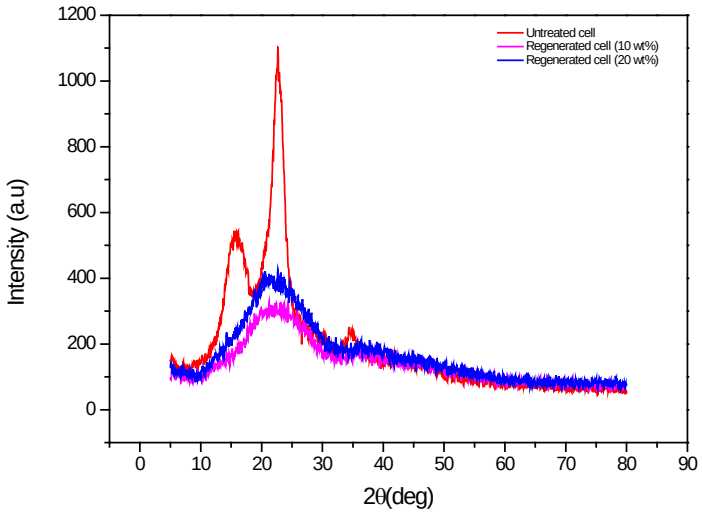

Figure 6. XRD diffraction for comparison the morphology of native cellulose (red) and regenerated cellulose (10wt % and 20wt %) in [3,5 ADMPy] Cl Ionic liquid at 120^{o}C.

The loss in crystallinity of cellulose samples upon dissolution in [3,5-ADMPy]Cl can be observed in the wide-angle X-ray diffraction spectra of native and regenerated cellulose samples. In order to further prove the dissolution of cellulose fibers in ionic liquids, the native cellulose 10 wt % and 20 wt% were taken to examine the morphology by wide-angle X-ray diffraction studies (Figure 6). The native cellulose shows three diffraction patterns at 2Ɵ 15.79, 22.68 and 34.6. The diffraction patterns of the 10 wt% and 20 wt% regenerated cellulose showed a broad peak at 2Ɵ of 22.68 degree, which correspond to the amorphous form of cellulose.[34-36] The diffraction pattern at 15.79 and 34.65 degrees corresponding to the crystallinity were absent. These observations clearly indicate that [3,5-ADMPy]Cl reduces strength of inter- and intra-molecular interactions upon dissolution of cellulose and thereby

reduces crystallinity.[37,38] The XRD result thus confirms the observations drawn from the SEM and NMR that crystallinity reduces during dissolution of cellulose in IL.

The thermal stability of native cellulose (C_1) and regenerated cellulose samples (C_2 and C_3) was studied by TGA and are shown in Figure 7. It is evident ~~from~~ when studying Figure 7 that native cellulose decompose at slightly higher temperature (325 °C) than regenerated cellulose samples (C_2 at 282 °C and C_3 at 278 °C). The reduction in thermal stability clearly indicate reduced crystallinity of cellulose samples and thus clearly supports NMR, XRD and SEM observations. The residue collected at 600 °C for the native and regenerated cellulose samples were 10%, and 18%, respectively. The difference in residue content of native and regenerated cellulose could possibly be due to the dissolution of minerals in ILs. Similar observations were noticed by Zhao *et al.* and Lan *et al.*[39,40]

The degree of polymerization of cellulose and the regenerated cellulose samples were observed by measuring viscosity using an Ubbelohde viscometer. Before DP measurements native and regenerated cellulose samples were dissolved in cupriethylenediamine (CED) hydroxide solution. The viscosity average DP of cellulose was estimated from its intrinsic viscosity [η]. The measurements showed that DP reduce from 1589 for native cellulose to 1325 for regenerated cellulose upon dissolution in [3,5-ADMPy]Cl. The lowering of DP post dissolution suggest that cellulose untangle during IL pretreatment.

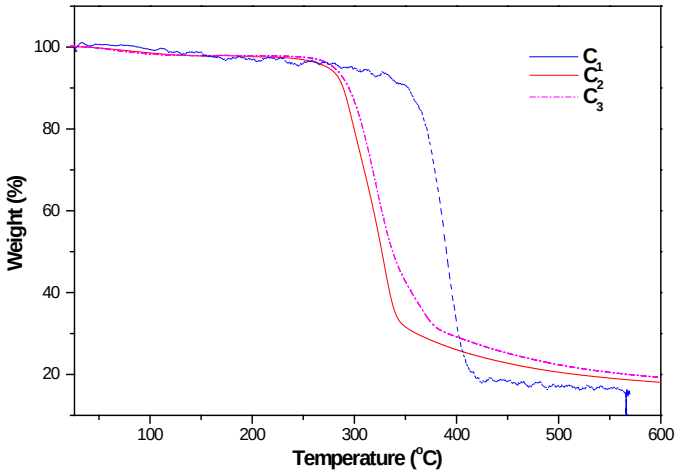

Figure 7. TGA for comparison the morphology of native cellulose (red) and regenerated cellulose (10wt % and 20wt %) in [3,5 ADMPy] Cl Ionic liquid at 120°C.

Conclusions

In this work, Lutidine-based ionic liquids were prepared and their potential ~~are~~ as cellulose solvents were tested ~~in dissolving cellulose samples~~ at different time-scales and temperatures (10 wt% sulfite cellulose in 8 min and 20 wt% cellulose in 12 min at 120 °C). The structure of the anion and position of the methyl groups over pyridinium cation were noted to affect the dissolution. Dissolution temperatures would be ~~chosen~~ kept below 110 °C to stabilize the DP of regenerated cellulose. After dissolution and regeneration in ionic liquid, the crystalline structure of cellulose was converted to amorphous cellulose. The thermal stability of cellulose regenerated was closer to the original cellulose, but the pyrolysis residues increased after dissolution and regeneration in ionic liquid. Therefore, [3,4-ADMPy]Cl was a promising solvent for cellulose with a low melting point, low viscosity and found to be a powerful, non-derivatizing single-component solvent for cellulose dissolution and processing of cellulose. The notable properties of the regenerated cellulose films are promising for applications in

transparent, biodegradable packaging and agricultural purpose as a substitute for poly propylene and poly ethylene.

Acknowledgments

The authors thank Kempe Foundations (Kempestiftelserna) for the financial support. The Wallenberg Wood Science Center Foundations and Bio4energy programme are acknowledged. This work is also part of the activities of the Johan Gadolin Process chemistry Centre at Åbo Akademi University.

Formatted: English (United Kingdom)

References

1. Ragauskas, A. J., Williams, C. K., Davison, B. H., Britovsek, G., Cairney, J., Eckert, C. A., Frederick, W. J., Hallett, J. P., Leak, D. J., Liotta, C. L., Mielenz, J. R., Murphy, R., Templer, R., Tschaplinski, T., Science, 2006, 311, 484−489.

2. Perlack, R. D., Stokes, B. J., U.S. Billion Ton Update: Biomass Supply for a Bioenergy and Bioproducts Industry; Oak Ridge National Laboratory: Oak Ridge, TN; U.S. Department of Energy: Washington, DC, 2011; l 227 pp, ORNL/TM-2011/224.

3. Himmel, M. E., Ding, S. Y., Johnson, D. K., Adney, W. S., Nimlos, M. R., Brady, J. W., Foust, T. D., Science, 2007, 315, 804−807.

4. Chen, G. Q., Patel, M. K., Chem. Rev., 2012, 112, 2082−2099.

5. George, J., Sabapathi, S. N., Nanotechnol Sci Appl., 2015; 8: 45–54.

6. Wojcieech, C., Dwight, R., Malcolm, B. J., Cellulose, 2004, 403-411.

7. Tsioptsias, C., Stefopoulos, A., Kokkinomalis, I., Papadopoulou, L., Panayiotou, C., Green Technology, 2008, 965-971.

8. Pinkert, A., Marsh, K. N., Pang, S., Ind. Eng. Chem. Res. 2010, 49, 11121 –11130.

9. Moutos, F. T., Freed, L. E., Guilak, F., Nat. Mater., 2007, 6, 162– 167.

10. Deshavath N. N., Mohan, M., Veeranki1, V. D., Goud, V. V., Pinnamaneni, S. R., Benarjee, T., Biotech (2017) 7:139.

Formatted: English (United States)

11. Timung, R., Deshavath, N. N., Goud, V. V., Dasu, V. V., Energy J., 2016, 2016, Article ID 8506214, 12 pages.

12. Teng, J., Ma, H., Wang, F., Wang, L., Li, X., *ACS Sustainable Chem. Eng.*, 2016, 4 (4), pp 2020–2026.

13. Heinze, T., Liebert, T., Prog. Polym. Sci. 2001, 26, 1689-1762.

14. Terbojevich, M., Cosani, A., Conio, G., Ciferri, A., Bianchi, E. Macromolecules 1985, 18, 640-646.

15. McCormick, C. L., Dawsey, T. R., Macromolecules 1990, 23, 3606-3610.

16. Nishio, Y., Manley, R. S. J., Macromolecules 1988, 21, 1270-1277.

17. Nishino, T., Matsuda, I., Hirao, K., Macromolecules 2004, 37, 7683-7687.

18. Williamson, S. L., Armentrout, R. S., Porter, R. S., McCormick, C. L., Macromolecules 1998, 31, 8134-8141.

19. Tamai, N., Tatsumi, D., Matsumoto, T., Biomacromolecules 2004, 5, 422-432.

20. Cai, J., Zhang, L., Liu, S., Liu, Y., Xu, X., Chen, X.. Macromolecules 2008, 41, 9345–9351.

21. Masson, J.-F., Manley, R. S. J., Macromolecules, 1991, 24, 5914-5921.

22. Masson, J.-F., Manley, R. S. J., Macromolecules 1991, 24, 6670-6679.

23. Teaca, C-A., Bodirlau, R., Spiridon, I., Rev. Roum. Chim., 2011, 56(1), 33-38.

24. Phillips, D. M., Drummy, L. F., Conrady, D. G., Fox, D. M., Naik, R. R., Stone, M. O., Trulove, P. C., De Long, H. C., Mantz, R. A., J. Am. Chem. Soc. 2004, 126, 14350-14351.

25. Seddon, K. R. J., Chem. Technol. Biotechnol. 1999, 68, 351-356.

26. Galinski, M., & Stepniak, I., J. Appl. Electro chemistry, 2009, 39, 1949–1953.

27. Brigouleix, C., Anouti, M., Jacquemin, J., Caillon-Caravanier, M., Galiano, H., & Lemordant, D., J. Phy. Chem B, 2010, 114, 1757–1766.

28. Swatloski, R.P., Spear, S.K., Holbrey, J.D., Rogers, R.D., J. Am. Chem. Soc. 2002, 124, 4974–4975.

29. Gericke, M., Fardim, P., Heinze, T., Molecules 2012, 17, 7458–7502.
30. Castelvetro, V., Geppi, M., Giaiacopi, S. and Mollica, G. Biomacromolecules, 2007, 8, 498–508.
31. Zuckerstätter, G., Schild, G., Wollboldt, P., Roeder, T., Weber, H. K., & Sixta, H. Lenzinger Ber., 2009, 87, 38–46.
32. Kamide, K., Okajima, K and Kowsaka, K, Polym. J, 24, 71–86, 1992.
33. Lateef, H., Grimes, S., Kewcharoenwong, P. and Feinberg, B., J. Chem. Technol. and Biotechnol, 2009, 84, 1818–1827.
34. Han, D and Yan, L., Carbohydrate Polymers, 2010, 79, 614–619.
35. Qi, H., Cai, C., Zhang, L and Kuga, S., Bio macromolecules, 2009, 10, 1597–1602.
36. Rahatekar, S. S., Rasheed, A. and Jain, R., Polymer, 2009, 50, 4577–4583.
37. Chen, H.-Z., Wang, N. and Liu, L.-Y., J. Chem. Technol and Biotechnol, 2012, 87, 1634–1640.
38. Zeronian, S. H. and Ryu, H.-S. J. Appl. Polym. Sci, 1987, 33, 2587–2604.
39. Dishun Zhaoa, He Li a, Juan Zhanga, Linlin Fua, Mengshuai Liua, Jiangtao Fua, Peibing Ren Carbohydrate Polymers, 2012, 87 1490– 1494.
40. Wu Lana, Chuan-Fu Liua, Feng-Xia Yuea, Run-Cang Suna, b, John F. Kennedyc Carbohydrate Polymers, 2011, 86 672– 677.

Graphical abstract